American Journal of Applied Sciences

Article

Control and Backbone Identification for the Resilient Recovery of a Supply Network Utilizing Outer Synchronization

Liang Geng [1] and Renbin Xiao [2,*]

[1] School of Science, Hubei University of Technology, Wuhan 430068, China
[2] School of Artificial Intelligence and Automation, Huazhong University of Science and Technology, Wuhan 430074, China

Abstract: The control and measurement for resilient recovery is important for a supply network facing disruption. Outer synchronization is useful for the supply network to recover to its scheduled state. In this paper, a dynamic model for a supply network is established, and measurement with memory of resilient recovery is proposed based on outer synchronization. An impulsive controller is designed to improve the control effectiveness. Afterwards, an algorithm is adopted to identify the resilient recovery backbone. Based on these factors, an efficient resilient recovery method considering cost is applied in the case study. This study improves the measurement and control of the supply network's resilient recovery through outer synchronization, and is easily integrated with practical problems to make better control decisions.

Keywords: outer synchronization; supply network; resilient recovery; adaptive impulsive control; backbone identification

1. Introduction

With the development of economic globalization, the increasing vulnerability of supply networks (SN) has drawn substantial attention to risk management [1,2]. Any event that negatively affects the information and material flow between suppliers and demanders should be considered as a risk to the disruption [3]. The resilience of a SN is a new concept related to its ability to mitigate vulnerability, which has been focused on in the last few years [4,5]. Merriam–Webster defines resilience as "the ability to recover or adjust easily to misfortune" [6]. A resilient SN is able to cope with (or react to) unexpected disruptions and recover quickly to the planned predisaster state [7], which results in the evolution of new practices to construct resilient SNs.

Network resilience can be defined in two fundamental dimensions: (i) vulnerability, or the lack of ability of a network to withstand disruptive events and maintain its maximum possible level of performance in the immediate aftermath of disruptions; and (ii) recoverability, or the ability of the network to return to a desired level of performance within a recovery time horizon [8]. These two dimensions describe components of robustness and rapidity in the resilience triangle. The resilience capacity of a system is defined as a function of three capacities: (i) absorptive capacity, or the extent to which a network is able to absorb shocks from disruptive events; (ii) adaptive capacity, or the extent to which a system can quickly adapt after a disruption by temporary means; and (iii) restorative capacity, or the extent to which the system can recover from a disruption or be reconstructed in the long-term [9].

Despite a growing number of research studies on SN resilience, there is still a lack of knowledge about resilient recovery. Moreover, few studies have attempted to measure and control resilient

recovery [10]. Considering all the above factors, this research attempts to seek answers to the following questions:

(1) What is the most efficient method of resilient recovery of the SN?
(2) How should the resilient recovery of the SN be measured?
(3) How should the backbone of the network for resilient recovery be identified?
(4) How should the resilient recovery of the SN be controlled?

The idea of network synchronization is to design appropriate controllers so that the network state can be tracked and synchronized to the target state. The study of synchronization is no longer limited to nodes within a network (internal synchronization), but also extends to synchronization between networks (outer synchronization) [11]. Outer synchronization can help the corresponding nodes to achieve the identical state. It is widely established that resilience means a return to a scheduled state [12]. Therefore, resilient recovery is a process of outer synchronization between the actual network after the disruption and the scheduled network before the disruption. Therefore, outer synchronization provides a feasible method for resilient recovery.

The effectiveness of resilient recovery measures is a key issue in engineering applications. However, most studies see the importance of network components as a standard for resilience measures [13], which is considered "memoryless", for the reason that this resilience standard does not take into account the previous information. It may have the same value of resilience with different restoration curves and different degrees of effectiveness. Therefore, resilience measures rely on the recovery time [6]. In this study, two indicators, namely recovery degree and recovery time, are introduced to quantify the effectiveness of resilient recovery. We propose a new method of outer synchronization-based recovery effectiveness measurement, which serves as the methodological background for the adoption of recovery measures.

In a dynamic and complex environment, there are many uncertain factors in the SN, such as the topological structure and order, production, and inventory parameters for different enterprises in case of disruption [14–16]. The research on complex networks and agent-based models provides help to solve this problem [17,18]. The outer synchronization problems for different network structures have been researched [19–21]. Zhang studied outer synchronization problems for uncertain parameters [22]. Later on, scholars investigated the various combinations of factors. Outer synchronization problems with different network structures and uncertain parameters have been studied [23–25]. Numerous technologies related to outer synchronization have been developed, for example pinning control [26,27] and impulse control [12,28]. The results of these important studies have laid a good foundation for further research studies about the practical application of outer synchronization. In the meantime, however, the question of how to design an effective outer synchronization controller considering the uncertainty of the SN isa pressing and challenging issue. In practice, connections between nodes may break due to interruption. Therefore, it is necessary to analyze the impact of topology on the resilient recovery of supply networks.

In fact, the nodes within the SN may become disconnected sometimes due to the disruption. Therefore, it is necessary to analyze the resilient recovery of the SN with the dynamic topology [29]. We found that many links are redundant for resilient recovery. Identifying and removing the redundant links for resilient recovery in the SN is one of the meaningful aspects in an application; analyzing resilient recovery strategies is another. The control efficiency is affected by not only resilient recovery effectiveness, but also cost control. In this paper, a control efficiency measurement method based on cost analysis is presented, which can be very helpful when controlling decision-making.

Based on the above discussions and previous studies [30], this paper aims at discussing outer synchronization-based resilient recovery measures with memory and control. The framework of this study is shown in Figure 1. The rest of the paper is organized as follows. In Section 2, we introduce a resilient recovery measurement based on the outer synchronization. In Section 3, the impulsive controller and the updated laws are designed. In Section 4, an algorithm is adopted to identify the

network backbone for resilient recovery and a measurement method of control efficiency is proposed considering cost analysis. In Section 5, the effectiveness of the method is verified by a case study. In the final section, a brief conclusion is given.

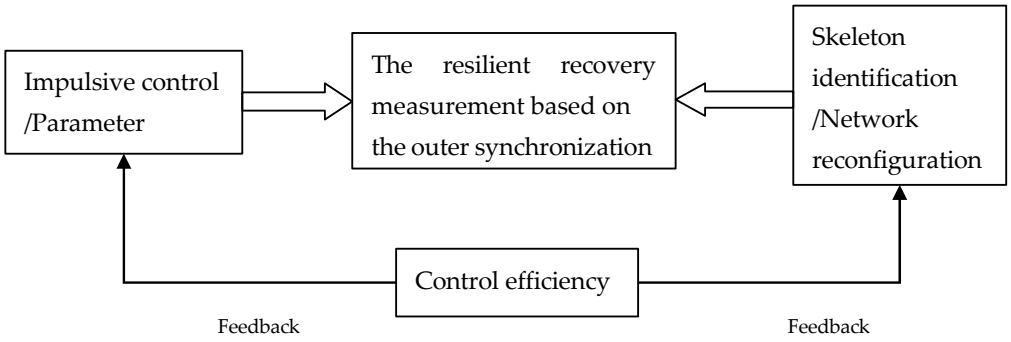

Figure 1. The framework of this study.

2. The Resilient Recovery of the SN Based on Outer Synchronization

2.1. Supply Network Model

The supply network (SN) is also known as the supply chain network. The SN can be simplified to a single supply chain when there is only one chain in it. In the supply chain, raw materials, intermediate materials, and finished goods are procured exclusively. A simple supply chain has been described previously by a set of differential equations [31–33]. This model can express the complex behavior of the supply chain perfectly. However, it cannot express complex network structures, meaning it is only suitable for a single-chain structure.

With the increase of supply objects and purchase objects, the supply chain structure is gradually upgraded to a network structure. The primary goal of the SN is to satisfy customer demands at the lowest cost.

From the perspective of structure, SN can be viewed as a collection of nodes $V = \{v_i\}$ (retailers, distributors, and manufacturers) and arcs $E = \{e_{ij}\}$ (the set of relations between the enterprise nodes). SN can be defined as a set of self-organizing agents that interact through a series of links. Therefore, SN can be expressed as $G = (V, E)$.

Since there isn't a central, authoritative organizing node, the SN is a self-organizing system. A dynamic SN is formed when each node is treated as a dynamic system. Each node has the behavior of ordering goods, production, and sales, whether it is a retailer, distributor, or manufacturer. In view of these studies [31–33], the status of each node in the SN can be described as

$$x_i(t) = [x_{i1}(t), x_{i2}(t), x_{i3}(t)]^T \tag{1}$$

The status of each enterprise can be expressed as Equation (2). The parameters are expressed in Table 1.

$$F_i(x_i(t), \alpha, \phi_i) = \begin{bmatrix} \dot{x}_{i1}(t) \\ \dot{x}_{i2}(t) \\ \dot{x}_{i3}(t) \end{bmatrix} = \begin{bmatrix} m(x_{i2}(t) - x_{i1}(t)) \\ rx_{i1}(t) - x_{i1}(t)x_{i3}(t) - x_{i2}(t) \\ x_{i1}(t)x_{i2}(t) - bx_{i3}(t) \end{bmatrix} = \begin{bmatrix} 0 \\ x_{i2}(t) - x_{i1}(t) \\ -x_{i1}(t)x_{i3}(t) - x_{i2}(t) \end{bmatrix} + \begin{bmatrix} 0 & 0 & 0 \\ 0 & 0 & x_{i1}(t) \\ 0 & x_{i3}(t) & 0 \end{bmatrix} \begin{bmatrix} m \\ -b \\ r \end{bmatrix} \tag{2}$$

Table 1. Parameters for the supply network.

Denotation	Definition
x_i	The status of node i
x_{i1}	Demand quantities for ordering
x_{i2}	Supply quantities for distribution
x_{i3}	Inventory for production
m	The dissatisfaction of ordering
r	Information distortion
b	The coefficients of safety stock

The variation of demand quantity $\dot{x}_{i1}(t)$ relates to the dissatisfaction m in the preceding period. The variation of the supply quantity $\dot{x}_{i2}(t)$ is influenced by the information distortion r and the supply quantities x_{i2} in the preceding period. It also needs to take into account both the demand quantities x_{i1} and the inventory x_{i3}. The variation of inventory $\dot{x}_{i3}(t)$ not only relates to the demand quantities x_{i1} and the supply quantities x_{i2}, but also depends on safety stock [34].

The state of each enterprise can be seen as a process, including order-taking, product-making, and goods distribution; similarly, the status of each node is affected by its neighboring nodes [35–37]. This is expressed by Equation (3).

$$\dot{x}_i(t) = F_i(x_i(t), \alpha, \phi_i) + \sum_{j \in N_i} g_{ij}\Gamma(x_j(t) - x_i(t))$$

$$\begin{bmatrix} \dot{x}_{i1}(t) \\ \dot{x}_{i2}(t) \\ \dot{x}_{i3}(t) \end{bmatrix} = \begin{bmatrix} m(x_{i2}(t) - x_{i1}(t)) \\ rx_{i1}(t) - x_{i1}(t)x_{i3}(t) - x_{i2}(t) \\ x_{i1}(t)x_{i2}(t) - bx_{i3}(t) \end{bmatrix} + \sum_{j \in N_i} g_{ij} \begin{bmatrix} c_1 & & \\ & c_2 & \\ & & c_3 \end{bmatrix} \begin{bmatrix} x_{j1}(t) - x_{i1}(t) \\ x_{j2}(t) - x_{i2}(t) \\ x_{j3}(t) - x_3(t) \end{bmatrix} \quad (3)$$

In Equation (3), the first item represents the state of node v_i itself, and the second item represents the impact on the state of node v_i by the neighboring nodes with a supply relationship. The state of each node is mainly adjusted by its own demand quantities x_{i1}, supply quantities x_{i2}, and inventory x_{i3}. In SN, there is not a one-to-one relationship, but a very complicated relationship.

There are interactions between supply quantities, demand quantities, and inventory. The supply quantity from v_i to v_j is not the demand quantity form v_j to v_i. Therefore, the state of the node is also adjusted by the state of the neighbor nodes with a supply relationship, using the second term.

The set of neighbors of node v_i is denoted by N_i. The neighbor of node v_i means that there is a supply relationship with the node v_i. The number of nodes v_j satisfying $j \in N_i$ shows how many nodes supply node v_i. The supply relationship may be one-to-one, or several-to-one, which is expressed by the adjacency matrix $G = [g_{ij}]$. When there is a business relationship between node v_i and v_j, $g_{ij} = 1$, otherwise $g_{ij} = 0$. G is symmetric and non-negative. The inner coupling matrix $\Gamma = diag(c_1, c_2, c_3)$ is a diagonal matrix to indicate coupling strength: where c is the coupling coefficient; c_1 represents the influence of neighbors of node x_i on the first component, demand quantities; c_2 represents the influence of neighbors of node x_i on the second component, supply quantities; c_3 represents the influence of neighbors of node x_i on the third component, inventory. The physical interpretation of the inner coupling matrix is the ability of mutual control between nodes.

For example, there is a supply relationship between a raw material node x_j and a factory node x_i. Since the raw material node x_j does not only supply to the factory node x_j, and the factory node x_i does not only demand from the raw material node x_j, the supply quantities of the raw material node x_j cannot be coupled to the demand quantities of the factory node x_i directly. In Equation (3), the demand quantities of the factory node x_i (x_{i1}) are related to the supply quantities of the raw material node x_j (x_{j2}) (i.e., $g_{ij} = 1$, x_{i1}–x_{j2}). Furthermore, in the first item of Equation (3), $F_j(x_j)$, the supply quantities of the raw material node x_j (x_{j2}) are related to the demand quantities of the raw material node x_j (x_{j1}) (i.e.,

x_{j2}–x_{j1}). So, the supply quantities of the raw material node are coupled to the supply quantities of the factory node x_i (i.e., x_{j2}–x_{j1}), which expresses the connections between nodes in Equation (3).

If the nodes are only interconnected through the demand relationship, then the nodes are coupled through the first component. In this scenario, $\Gamma = diag(c, 0, 0)$.

The configuration matrix $A = [a_{ij}]$ is used, therein $a_{ij} = -g_{ij}$ $(i \neq j)$, $a_{ii} = \sum_{j}^{N} g_{ij}$, then Equation (3) becomes Equation (4)

$$\dot{x}_i(t) = f_{1i}(x_i(t), \phi_i) + f_{2i}(x_i(t), \phi_i)\alpha + \sum_{j \in N_i} a_{ij}\Gamma x_j(t) \tag{4}$$

Therein, α is the vector with scheduled parameters, ϕ_i is the scheduled status, f_{1i} is the function without parameters, and f_{2i} is the function with parameters. The validity of the proposed SN model has been presented in our previous study [30].

2.2. Resilient Recovery Based on Outer Synchronization

The actual SN after disruption acts as the response network, shown as Equation (4). Therein, $A \neq B$ ($A = [a_{ij}]$, $B = [b_{ij}]$) as the structure has been changed, the status ψ_i of the actual SN is changed, so u_i is the control function. Here, $\bar{\alpha}$ is the vector with the unknown parameter, which means that the original schedule is changed.

$$\begin{aligned} \dot{y}_i(t) &= F_i(y_i(t), \alpha, \psi_i) + \sum_{j \in N_i} b_{ij}\Gamma y_j(t) + u_i \\ &= f_{1i}(y_i(t), \psi_i) + f_{2i}(y_i(t), \psi_i)\bar{\alpha} + \sum_{j \in N_i} b_{ij}\Gamma y_j(t) + u_i \end{aligned} \tag{5}$$

Definition 1. *Outer synchronization is achieved between the actual network and scheduled network; for any initial values ϕ_i and ψ_i, then parameters are α and $\bar{\alpha}$, such that*

$$\lim_{t \to \infty} \|e_i\| = \lim_{t \to \infty} \| y_i(t, \bar{\alpha}, \psi_i) - x_i(t, \alpha, \phi_i) \| = 0$$

where e_i is an synchronization error [38].

The outer synchronization between the actual network and the corresponding scheduled network is shown in Figure 2a. Particularly, if $m = 10$, $r = 28$, $b = 8/3$, the system is typically in a state of chaos, as shown in Figure 2b.

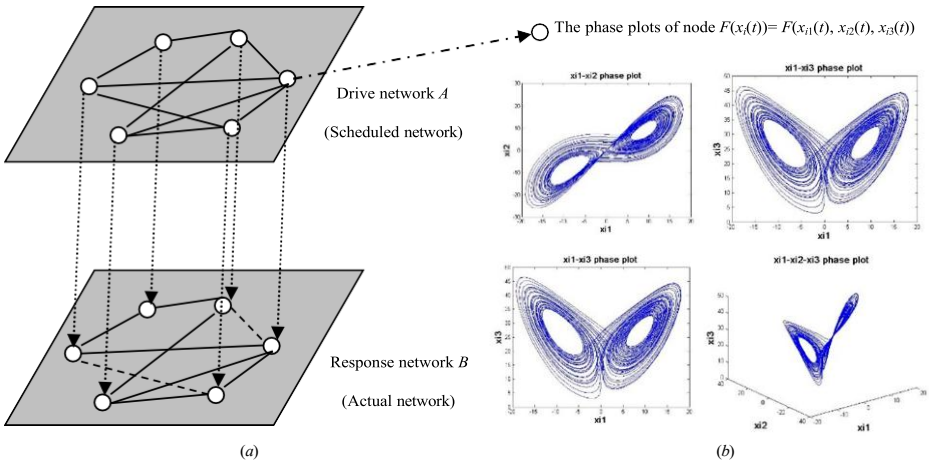

Figure 2. Synchronization of the supply network (SN). (**a**) Outer synchronization, (**b**) The status of node.

As shown in Figure 3, the status of node y_i synchronizes to the status of corresponding node x_i. The status in the actual network fluctuates near the scheduled status and tends to the status in the scheduled network.

Definition 2. *Resilient recovery is a process of outer synchronization between the actual network and scheduled network.*

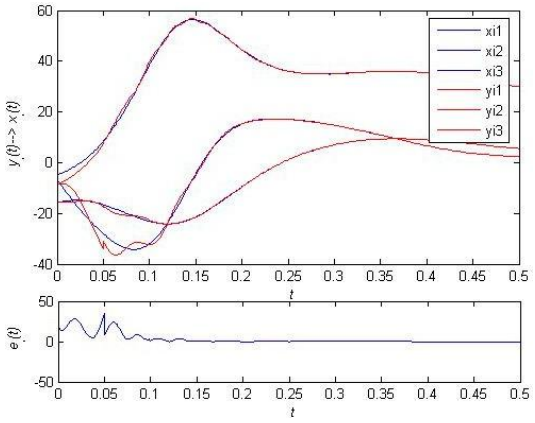

Figure 3. Synchronization of node i ($y_{i1} \rightarrow x_{i1}$, $y_{i2} \rightarrow x_{i2}$, $y_{i3} \rightarrow x_{i3}$, $e_i \rightarrow 0$).

2.3. The Resilient Recovery Measurement Based on the Outer Synchronization Error

Resilience is the ability to accomplish the original plan in any case [39]. As shown in Figure 4, a quantifiable and time-dependent performance function is the basis for the measurement of the resilience [6,13,40,41]. The dotted curve $FT(t)$ denotes the targeted performance function of SN if not affected by disruption. The disruption deteriorates the performance to the level $F(t_d)$ at time t_d. Then, the performance function of SN $F(t)$ will be improved by recovery action and reach the targeted level $FT(t)$ at a later time t_r.

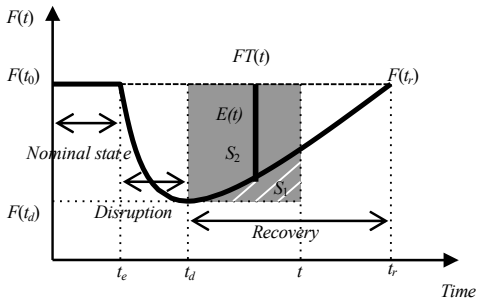

Figure 4. Illustration of the resilient recovery measurement.

Let $R1(t)$ be the resilient recovery ratio of SN at time t ($t > t_d$). $R1(t)$ describes the cumulative functionality that has been restored at time t, normalized by the expected cumulative functionality if the SN has not been affected by disruption. $R1(t)$ is given as Equation (6), where $R1(t)$ is quantified by the ratio of the area with diagonal stripes S_1 to the area of the shaded part S_2 [6].

$$R1(t) = \frac{\int_{t_d}^{t} [F(\tau) - F(t_d)]d\tau}{\int_{t_d}^{t} [FT(\tau) - F(t_d)]d\tau}, \quad t \geq t_d \tag{6}$$

Outer synchronization error $e_i \rightarrow 0$ shows that the actual status restores itself to the scheduled status. That is to say, the smaller the outer synchronization error, the better the resilient recovery.

Total outer synchronization error of all nodes is expressed as Equation (7):

$$E(t) = \sqrt{\sum_{i=1}^{N} [(x_{i1}(t) - y_{i1}(t))^2 + (x_{i2}(t) - y_{i2}(t))^2 + (x_{i3}(t) - y_{i3}(t))^2]} \quad (7)$$

The outer synchronization error of all nodes $E(t) = |F(t) - FT(t)|$ can be used to measure the resilience.

Taking advantage of the outer synchronization error, a function for the assessment of the resilience is illustrated in Figure 5. It is a quantifiable and time-dependent performance function, also known as the resilient recovery ratio, which can be measured by $R(t)$:

$$R(t) = 1 - \frac{\int_{t_d}^{t} E(\tau)d\tau}{\int_{t_d}^{t} ET(\tau)d\tau}, \; t \geq t_d \quad (8)$$

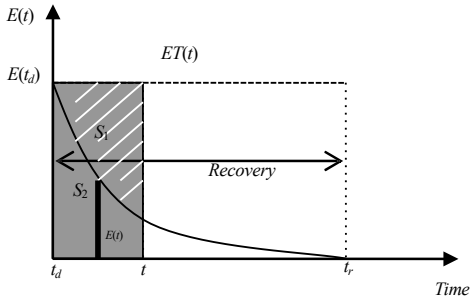

Figure 5. Measurement of resilient recovery utilizing outer synchronization error.

Equation (8) focuses on the resilient recovery in the range of [0, 1]. $R(t) = 0$ when $E(t) = ET(t)$. This means that SN has not recovered from its disrupted state (there has been no "resilience" action); $R(t) = 1$ when $E(t) = 0$, which corresponds to the ideal case, where SN recovers to its scheduled state immediately after disruption.

This resilient recovery quantification is capable of measuring both the magnitude and rapidity of recovery. Moreover, this measurement of resilient recovery is not memoryless, since it considers the cumulative recovery of the functionality.

3. Design of Adaptive-Impulsive Controller

Assumption 1. *For any $x_i(t) = (x_{i1}(t), x_{i2}(t), \ldots, x_{in}(t))^T$ and $y_i(t) = (y_{i1}(t), y_{i2}(t), \ldots, y_{in}(t))^T$, there exists a positive constant $L_i > 0$, such that $\|F_i(t, y_i(t), \alpha_i) - F_i(t, x_i(t), \alpha_i)\| \leq L_i \| y_i(t) - x_i(t)\|$.*

Our goal is to design an adaptive pulse controller user interface(UI) that allows the actual network to be asymptotically synchronized with the scheduled network to reduce costs [21,42]. The response network is designed as

$$\begin{cases} \dot{y}_i(t) = f_{1i}(y_i(t)) + f_{2i}(y_i(t))\bar{\alpha} + \sum_{j=N_i} b_{ij}\Gamma y_j(t) + u_i \; t \neq t_k, \\ \Delta y_i(t^+) = B_{ik}e_i(t), \quad t = t_k, k = 1, 2, \cdots, \\ y_i(t_0^+) = y_{i0} \end{cases} \quad (9)$$

where $\bar{\alpha}$ is the estimation of the unknown α, B_{ik} is the feedback matrix of node i received at impulsive moment t_k, u_i is the adaptive controller received by the node i, and:
$y_i(t_k^+) = \lim_{t \to t_k^+} y_i(t)$, $y_i(t_k^-) = \lim_{t \to t_k^-} y_i(t)$, $\Delta y_i(t_k^+) = y_i(t_k^+) - y_i(t_k^-)$. *Here, t_k satisfies $0 \leq t_1 < t_2 < \ldots < t_k < \ldots$, and $\lim_{k \to \infty} t_k = +\infty$.*

Theorem 1. *Supposing that Assumption 1 holds, then:*

Let $\kappa = \lambda_{\max}\left(\frac{1}{2}((B \otimes \Gamma) + (B \otimes \Gamma)^T)\right)$, $\iota = \lambda_{\max}\left(\frac{1}{2}((A \otimes \Gamma) + (A \otimes \Gamma)^T)\right)$, $v = (L - g + \kappa + \iota) < 0$, *and* $\chi = \max(v, -\mu) < 0$. *If* $\lambda_{\max}[(I + B_{ik})^T(I + B_{ik})] < 1$ *and* $\exists \xi > 1$, *then* $2\chi\tau_k + \ln(\xi) < 0$.

$$\begin{cases} u_i(t) = -g_i e_i - \mu \|\alpha_i - \alpha\|^2 \frac{e_i}{\|E\|^2} - \sum_{j=1}^{N} b_{ij}\Gamma x_j(t) + \sum_{j=1}^{N} a_{ij}\Gamma y_j(t) \\ \dot{g}_i = k_i \|e_i\|^2 \\ \dot{\alpha}_i = -f_2^T(y_i(t))e_i(t) \end{cases} \tag{10}$$

The drive system in Equation (4) and the respond system in Equation (5) can achieve outer synchronization.

The controller u_i *is designed as the first equation in Equation (10), where* g_i *is the coefficient for control gain and* μ *is the coefficient for parameter identification. The two sum terms are the control of structure change. The updating laws of control gain and unknown parameters are designed in the last two equations of Equation (10), where* k_i *is the control strength and* f_{2i} *is the part associated with parameters in* F_i.

Proof. Consider the following Lyapunov function:

$$\begin{aligned} V &= \frac{1}{2}\|E(t)\|^2 + \frac{1}{2}\|\alpha - \alpha\|^2 \\ &= \frac{1}{2}\sum_{i=1}^{N} e_i^T e_i + \frac{1}{2}\sum_{i=1}^{N} (\alpha_i - \alpha_i)^T(\alpha_i - \alpha_i) \end{aligned} \tag{11}$$

By the synchronization error $e_i(t) = y_i(t) - x_i(t)$, we have

$$\dot{e}_i(t) = (f_{1i}(y_i(t) - f_{1i}(x_i(t)) + (f_{2i}(y_i(t)\alpha - f_{2i}(x_i(t)\alpha) + \sum_{j=N_i} (b_{ij}\Gamma y_j(t) - a_{ij}\Gamma x_j(t)) + u_i(t)$$

Then

$$\dot{V} = \sum_{i=1}^{N} e_i^T e_i + \sum_{i=1}^{N} \dot{\alpha}_i^T(\alpha_i - \alpha_i)$$

$$\begin{aligned} \dot{V} = & \sum_{i=1}^{N} e_i^T[(f_{1i}(y_i(t) - f_{1i}(x_i(t)) + (f_{2i}(y_i(t)\alpha - f_{2i}(x_i(t)\alpha + \sum_{j=N_i} b_{ij}\Gamma y_j(t) - \sum_{j=N_i} a_{ij}\Gamma x_j(t) - \sum_{j=N_i} b_{ij}\Gamma x_j(t) \\ & + \sum_{j=N_i} a_{ij}\Gamma y_j(t) - g_i e_i - \mu\|\alpha - \alpha\|^2 \frac{e_i}{\|E\|^2}] + \sum_{i=1}^{N} \dot{\alpha}^T(\alpha - \alpha) \\ \dot{V} = & \sum_{i=1}^{N} e_i^T[(f_{1i}(y_i(t) - f_{1i}(x_i(t)) + (f_{2i}(y_i(t)\alpha - f_{2i}(x_i(t)\alpha + \sum_{j=N_i} b_{ij}\Gamma e_j(t) + \sum_{j=N_i} a_{ij}\Gamma e_j(t) \\ & - g_i e_i - \mu\|\alpha - \alpha\|^2 \frac{e_i}{\|E\|^2}] + \sum_{i=1}^{N} \dot{\alpha}^T(\alpha - \alpha) \\ \dot{V} = & \sum_{i=1}^{N} e_i^T[f_{1i}(y_i(t)) - f_{1i}(x_i(t))] + \sum_{i=1}^{N} e_i^T[f_{2i}(y_i(t))\alpha - f_{2i}(x_i(t))\alpha] + \sum_{i=1}^{N}\sum_{j=1}^{N} e_i^T b_{ij}\Gamma e_i(t) \\ & + \sum_{i=1}^{N}\sum_{j=1}^{N} e_i^T a_{ij}\Gamma e_i(t) - \sum_{i=1}^{N} e_i^T g_i e_i - \mu\sum_{i=1}^{N} \|\alpha - \alpha\|^2 e_i^T \frac{e_i}{\|E\|^2} + \sum_{i=1}^{N} \dot{\alpha}^T(\alpha - \alpha) \end{aligned} \tag{12}$$

Noticing that $\dot{\alpha} = -f_{2i}^T(y_i(t))e_i(t)$, then $\dot{\alpha}^T = -e_i(t)^T f_{2i}(y_i(t))$

We have

$$\begin{aligned} & \sum_{i=1}^{N} e_i^T[f_{1i}(y_i(t)) - f_{1i}(x_i(t))] + \sum_{i=1}^{N} e_i^T[f_{2i}(y_i(t))\alpha - f_{2i}(x_i(t))\alpha] + \sum_{i=1}^{N} \dot{\alpha}^T(\alpha - \alpha) \\ = & \sum_{i=1}^{N} e_i^T[f_{1i}(y_i(t)) - f_{1i}(x_i(t))] + \sum_{i=1}^{N} e_i^T[f_{2i}(y_i(t))(\alpha - \alpha)] + \sum_{i=1}^{N} -e_i(t)^T f_{2i}(y_i(t))(\alpha - \alpha) \\ = & \sum_{i=1}^{N} e_i^T[f_{1i}(y_i(t)) - f_{1i}(x_i(t))] \\ \leq & L\sum_{i=1}^{N} e_i^T e_i \end{aligned} \tag{13}$$

where $L = max\{L_i\}$.

Noticing that $\sum_{i=1}^{N} e_i^T \frac{e_i}{\|E\|^2} = 1$, we have

$$\begin{aligned} &-\sum_{i=1}^{N} e_i^T g_i e_i - \mu \sum_{i=1}^{N} \|\alpha - \alpha_i\|^2 e_i^T \frac{e_i}{\|E\|^2} \\ &= \sum_{i=1}^{N} -g_i \|e_i\|^2 - \mu \sum_{i=1}^{N} \|\alpha - \alpha\|^2 e_i^T \frac{e_i}{\|E\|^2} \\ &= \sum_{i=1}^{N} -g \|e_i\|^2 - \mu \sum_{i=1}^{N} \|\bar{\alpha} - \alpha\|^2 \end{aligned} \tag{14}$$

Equation (11) can be simplified as

$$\begin{aligned} \dot{V} &\le L \sum_{i=1}^{N} e_i^T e_i + \sum_{i=1}^{N} \sum_{j=1}^{N} e_i^T b_{ij} \Gamma e_i(t) + \sum_{i=1}^{N} \sum_{j=1}^{N} e_i^T a_{ij} \Gamma e_i(t) + \sum_{i=1}^{N} -g \|e_i\|^2 - \mu \sum_{i=1}^{N} \|\bar{\alpha} - \alpha\|^2 \\ &\le (L - g) E^T(t) E(t) + E^T(t)(B \otimes \Gamma) E(t) + E^T(t)(A \otimes \Gamma) E(t) - \mu \sum_{i=1}^{N} \|\bar{\alpha} - \alpha\|^2 \end{aligned} \tag{15}$$

where $\otimes$ is the Kronecker product.

$$\begin{aligned} \dot{V}(t) &\le (L - g) E^T(t) E(t) + \left[\frac{(B \otimes \Gamma) + (B \otimes \Gamma)^T}{2} + \frac{(A \otimes \Gamma) + (A \otimes \Gamma)^T}{2} \right] \times E^T(t) E(t) - \mu \sum_{i=1}^{N} \|\bar{\alpha} - \alpha\|^2 \\ &\le (L - g + \kappa + \iota) \times E^T(t) E(t) - \mu \sum_{i=1}^{N} \|\bar{\alpha} - \alpha\|^2 \\ &\le 2\chi V(t) \end{aligned}$$

where $\kappa = \lambda_{\max}\left\{\frac{1}{2}((B \otimes \Gamma) + (B \otimes \Gamma)^T)\right\}$, $\iota = \lambda_{\max}\left\{\frac{1}{2}((A \otimes \Gamma) + (A \otimes \Gamma)^T)\right\}$, $v = (L - g + \kappa + \iota) < 0$, and $\chi = \max(v, -\mu) < 0$.

This implies that

$$V(t) \le V(t_{k-1}^+) e^{2\chi(t - t_{k-1})}, \ t = (t_{k-1}, t_k] \tag{16}$$

When $t = t_k$, then:

$$\begin{aligned} e_i(t_k^+) &= y_i(t_k^+) - x_i(t_k^+) = y_i(t_k) + B_{ik}(t_k) e_i(t_k) - x_i(t_k) = (I + B_{ik}) e_i(t_k) \\ V(t_k^+) &= \frac{1}{2} \sum_{i=1}^{N} e_i^T(t_k)(I + B_{ik})^T (I + B_{ik}) e_i(t_k) + \frac{1}{2} \sum_{i=1}^{N} (\bar{\alpha} - \alpha)^T (\bar{\alpha} - \alpha) \\ &\le V(t_k) \end{aligned} \tag{17}$$

Due to $\lambda_{max}[(I + B_{ik})^T (I + B_{ik})] < 1$.

From Equations (16) and (17), there is

$$V(t) \le V(t_0^+) e^{2\chi(t - t_0)}, \ t = (t_{k-1}, t_k] \tag{18}$$

By Theorem 1, we know that $e^{2\chi\tau_k} < \frac{1}{\xi}$, $k = 1, 2, \cdots$.

Thus, the inequality in Equation (18) can be further rewritten as

$$\begin{aligned} V(t) &\le V(t_0^+)(e^{2\chi\tau_1}) \cdots (e^{2\chi\tau_k}) e^{2\chi(t - t_k)} \\ &< V(t_0^+) \frac{1}{\xi^k} e^{2\chi\tau_{k+1}} \end{aligned} \tag{19}$$

We have $V(t) \to 0, (k \to \infty)$. That is, $e_i(t) \to 0$ and $\bar{\alpha} \to \alpha$. This means the outer synchronization is realized between the drive network in Equation (4) and the response network in Equation (5). Then, the proof work is completed. □

4. Application of the Method

4.1. Network Skeleton Identification Forresilient Recovery

As shown in Figure 6, the network's resilient recovery ability will stay almost unchanged if the link between 1 and 4 (1–4) is removed (network a → network b). The analysis indicates that every link has unequal contribution to the resilient recovery ability. In other words, the resilient recovery of SN is hardly affected if certain links are removed. It has been discovered that many links in the network are actually redundant for resilient recovery, known as redundant links. The backbone of resilient recovery is the minimal network maintaining resilient recovery ability, which is the network when the redundant links have been removed. Disruption may occur anywhere in a SN, so the question of how to identify the backbone of resilient recovery is of great importance.

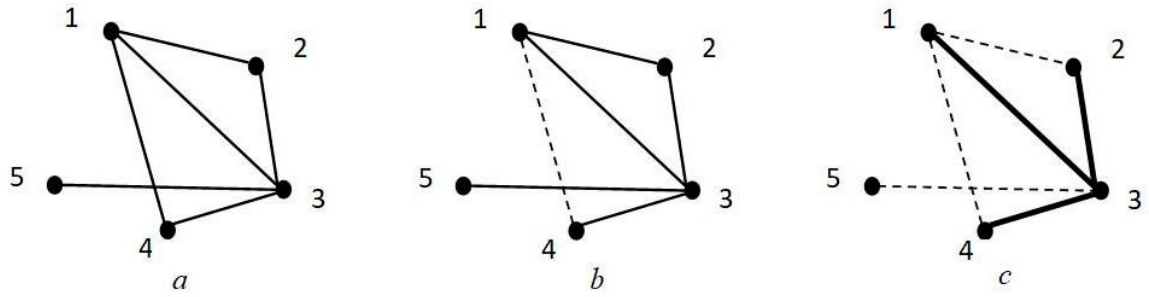

Figure 6. Skeleton identification for resilient recovery. (**a**) network a, (**b**) network b, (**c**) network *c*.

In order to remove the redundant links, a greedy algorithm is designed based on $R(t)$ in Equation (8), in which the resilient recovery ratio of the original SN is expressed as $R^{(0)}$, and the resilient recovery ratio of the reduced network after removing l links is denoted as $R^{(l)}$ [43].

$$\Delta R = |R^{(l)} - R^{(l-1)}| \tag{20}$$

Then, one can calculate ΔR of each remaining link and select the link with lowest ΔR to be actually removed from the network. Then, continue to remove links until $R^{(l)}$ falls below 98% of $R^{(0)}$ and the obtained network is denoted as the network backbone of resilient recovery. As shown in Figure 5 (network *c*), the network backbone of resilient recovery is obtained when the redundant links (1–4, 1–2, 3–5) are removed.

4.2. Control Efficiency Analysis

Two factors are introduced to measure the efficiency of the control $R_C(t)$. One is the liveness of resilient recovery $R(t)$, which is proportional to $R_C(t)$. The other is the controlling cost $C(t)$, which is inversely proportional to $R_C(t)$. The control efficiency $R_C(t)$ is represented as Equation (20), which can be applied to compare SN recovery strategies.

$$R_C(t) = R(t)/C(t) \tag{21}$$

The supply chain strategies are taken from [44]. There are five recovery strategies in our model (listed below), and the corresponding control costs are shown in Figure 7.

(1) Emergency management costs. The parameter g shows the capability of emergency management.

(2) Strategy adjustment costs. The parameter μ used to identify $\bar{\alpha}$ indicates the capability for strategy adjustment.
(3) Coupled node controlling costs. The coupling relationship will be changed by the structural changes. The parameter Γ is used to control the heterogeneous coupled nodes.
(4) Incentive mechanism costs. The feedback matrix B_{ik} and pulse period t are concerned with the intensity and frequency of the incentive mechanism, respectively.
(5) Reconstruction costs.

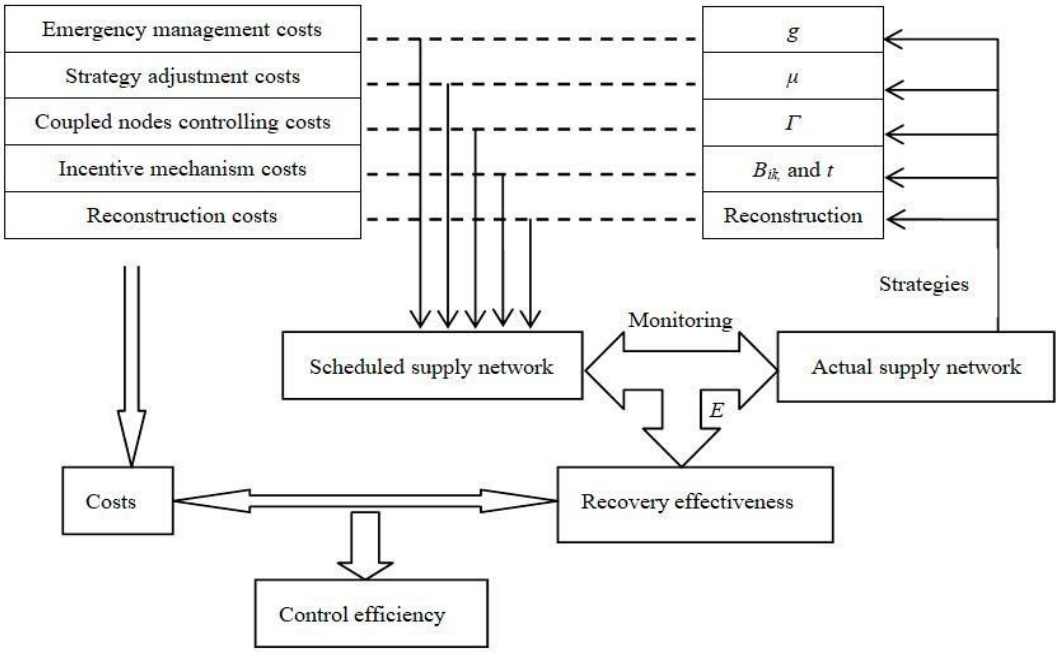

Figure 7. Measurement of control efficiency.

5. A Case Study in Engineering Application

5.1. The Experimental Background

A SN is used in the case study [45]. This network structure has representative characteristics. The initial scheduled network A is seen as the drive network, as shown in Figure 8. Based on previous studies, we use empirical data [30]. The supply network contains raw materials suppliers (S), factories (P), warehouses (W) and markets (M). The status of the node is initialized randomly. The main values of the parameters α (m; r; b; Γ) which used in the case study are shown in Table 2.

Table 2. The main values used in the case study.

Type	S	P	W	M	m	r	b	Γ
values	11	3	5	18	10	28	2.6	diag(5, 5, 5)

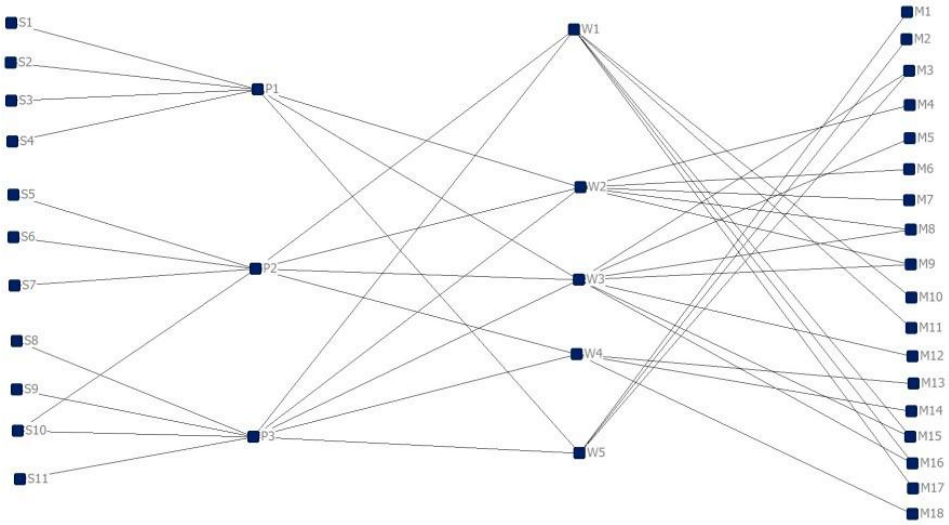

Figure 8. Structure of a European supply network *A*.

5.2. The Effectiveness of the Resilient Recovery Method based on Outer Synchronization

Assuming that a failure occurs in the enterprise node W_1, this causes a pause of the contacts in $W_1\_M_{10}$, $W_1\_M_{11}$, and $W_1\_P_2$. In this disruption, the network structure is changed, along with the status values and the parameters. The supply network *B* acts as the response network, where $B \neq A$. Assuming that $\bar{\alpha}(m, r, b)$ are unknown after the disruption, the status of the response network is initialized randomly.

An adaptive impulsive controller is adopted in Section 3. Assuming that the period of impulse control $t = 0.05$, the feedback matrix $B_{ik} = diag[-0.5, -0.5, -0.5]$, the inner coupling matrix $\Gamma = diag(0.2, 0.2, 0.2)$, and the controller's parameters are $L = 1$, $g = 7$, $\mu = 1.5$, $t_k = 0.05$. By using MATLAB Toolbox, we can get $\kappa = 2.8419$, $\iota = 3.0448$, $\lambda_{max} = 0.25 < 1$, $v = (L - g + \kappa + \iota) = -0.1133 < 0$, and $\chi = \max(v, -\mu) = -1.5 < 0$. $\exists \xi > 1$, such that $2\chi\tau_k + \ln(\xi) < 0$. Then, Theorem 1 can be satisfied and the network can achieve outer synchronization.

The synchronization errors are shown in Figure 9. Here, $e_i \to 0$ after 3 impulse periods; $e_i(t)$ reduces obviously at times $t = 0.05$, $t = 0.1$, and $t = 0.15$. This means that the impulsive control can recover rapidly.

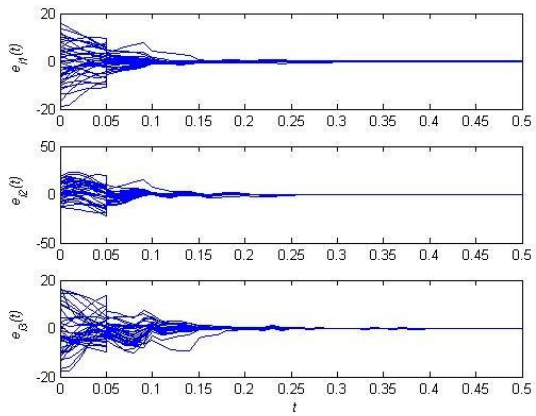

Figure 9. Error $e_i(t)$.

The parameter identification of the SN is realized in Figure 10. The uncertain parameter $\bar{\alpha}$ in the actual network (as in Equation (4)) will adjust adaptively in the process of outer synchronization and approach $\alpha(m = 10; r = 2.6; b = 28)$ in the scheduled network (Equation (3)). The parameter

identification is the process of adaptive adjustment. The synchronization error of all nodes $E(t)$ is presented in Figures 11 and 12, which can be used to measure the resilient recovery of the SN. Figure 11 shows that the SN can be restored to a certain extent without parameter identification (i.e., initial values $\overline{\alpha}(m = -7.5029, r = -7.4705, b = -9.6804)$ are not adjusted). The SN can be restored more easily with parameter identification than without parameter identification. This shows that the adaptive capacity of the SN will be better with parameter identification. As shown in Figure 12, the degree of resilient recovery $R(t)$ is measured at the time $t = 0.3$, where $R(0.3) = 0.7109$.

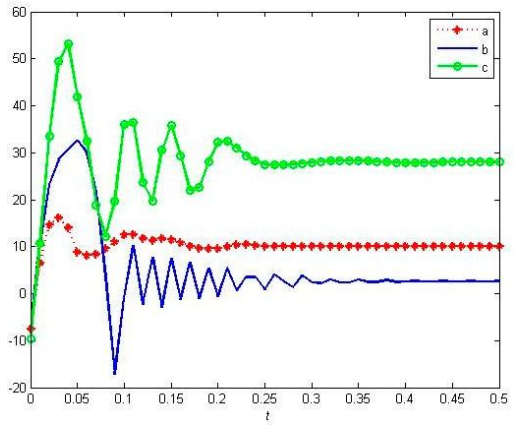

Figure 10. Of system parameters.

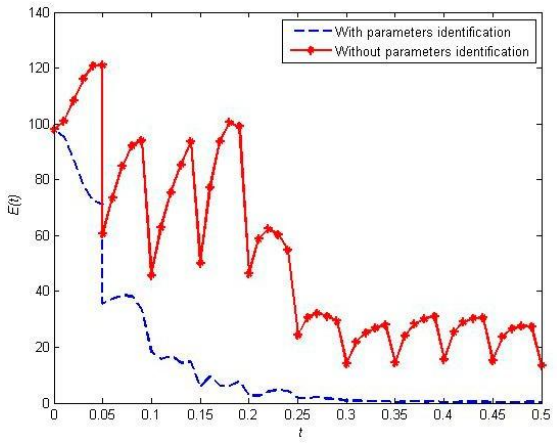

Figure 11. Effectiveness of parameters identification.

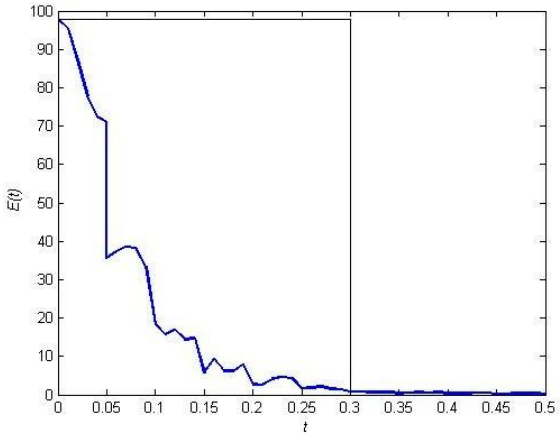

Figure 12. Resilient recovery measurement based on $E(t)$.

Through the above discussion, we can see that the SN utilizing outer synchronization can effectively be restored to the scheduled state and that the resilient recovery measurement is feasible and valid.

5.3. Backbone Identification for the Resilient Recovery of the Supply Network

We have proposed how the network backbone for resilient recovery can be identified by using the greedy algorithm in Section 4.1. Based on the correlation between recovery rate and time, the resilient recovery ratio $R(t)$ at time t = 0.15 is taken as the standard for comparisons (shown in Figure 13). The initial recovery ratio $R(0)$ = 0.5583. The recovery ratio should be kept at more than 98% of the standard value after the redundant links are removed. The sequence of removing redundant links and the corresponding recovery ratio are shown in Table 3. The backbone of the resilient recovery is showed in Figure 14.

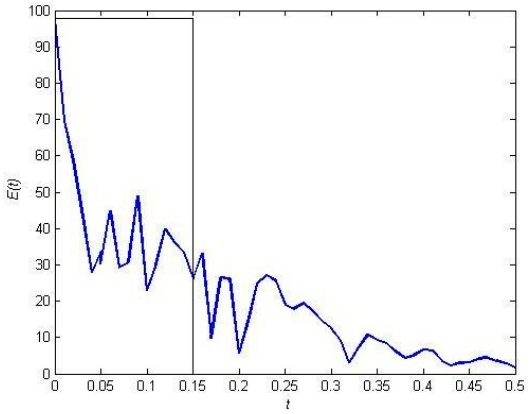

Figure 13. Resilient recovery ratio $R(t)$ at time t = 0.15, corresponding to Figure 4.

Table 3. Sequence for removing redundant links and the corresponding recovery ratio.

1	**2**	**3**	**4**	**5**	**6**	**7**	**8**	**9**
M8-W3	W1-P2	W3-P2	M3-W5	W2-P2	W3-P3	M16-W1	M9-W2	W2-P3
0.5583	0.5585	0.5582	0.5582	0.5579	0.5581	0.5585	0.5582	0.5579
10	**11**	**12**	**13**	**14**	**15**	**16**	**17**	**18**
P1-S2	M16-W3	M15-W3	M12-W3	P3-S10	M10-W1	M13-W4	W4-P3	W5-P3
0.5577	0.5573	0.5559	0.5564	0.5552	0.5524	0.5499	0.5482	0.5456

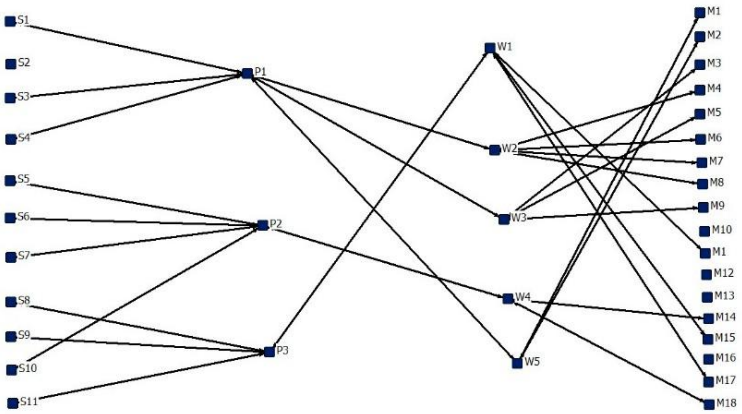

Figure 14. Backbone of resilient recovery.

We start again from the initial scheduled network A and remove these links in random order. This shows that the removal sequence does not significantly influence the resilient recovery ratio $R(t)$, confirming that these links are redundant for the resilient recovery. Furthermore, experiments show that the backbone of the network recovery is related to the initial value. That is to say, the different initial values will obtain different network backbones.

In order to show the effect of the backbone identification on the resilient recovery, the following cases are compared, as shown in Table 4. In the experiments, the above initial value is adopted, yet the resilient recovery ratio $R(0.3)$ at time $t = 0.3$ in different disrupted networks is calculated.

Table 4. Resilient recovery rate $R(t)$ in the cases.

	Network Structure	Remove Links	$R(0.3)$
	Backbone	18 links, as in Table 2	0.7127
Case 1	Network 1	W3-M3, W3-M5, W3-P1, W1-M11, W1-M17, W1-P3	0.7132
	Network 2	W3-M8, W3-M12, W3-P2, W1-M10, W1-M16, W1-P2	0.7250
Case 2	Network 3	P2-S5, P2-S6, P2-W4, W2-P1, W2-P6, W2-M8	0.7205
	Network 4	P3-S10, P3-W2, P3-W3, W2-P2, W2-M9, W3-M12	0.7236
Case 3	Network 5	W5-M1, W5-M2, W5-P1, W1-M11, W1-M15, W1-P3	0.7073
	Network 6	W5-M3, W5-P3, P3-W4, P3-W3, P3-W2, P2-W1	0.7253

Case 1: In network 1, a disruption occurs in the enterprise nodesW_1 and W_3, causing six links that belong to the backbone to be removed. In network 2, a disruption still occurs in the enterprise nodesW_1 and W_3, causing six redundant links (not belonging to the backbone) to be removed, R (network 1) < R (network 2), as shown in Figure 14.

Case 2: In network 3, a disruption occurs in the enterprise nodesW_2 and P_2, causing six links that belong to the backbone to be removed. In network 4, a disruption still occurs in the enterprise nodesW_2 and P_2, causing six redundant links to be removed, R (network 3) < R (network 4), but the difference is not obvious.

Case 3: In network 5, a disruption occurs in the enterprise nodesW_1 and W_5, causing six links that belong to the backbone to be removed. In network 6, a disruption still occurs in the enterprise nodesW_1, W_5, and P_3, causing six redundant links to be removed, R (network 5) < R (network 6), where the difference is obvious.

In networks 2, 4, and 6, the removal of six redundant links has little effect on resilient recovery, despite their different locations. In networks 1, 3, and 5, the removal of 6 backbone links exerts greatly effect on resilient recovery. It can be seen that the position of the removed links has different effects on resilient recovery and there are also primary and secondary points in the backbone links. For example, the removed links in network 5 are more important than the removed links in network 3.

As Figure 15 shows, removing links belonging to the backbone causes greater damage than removing the other redundant links. Therefore, it is very important to identify the network backbone during resilient recovery.

5.4. Control Effect Analysis for Resilient Recovery

In this case study, the following disruption is considered. A fire occurs in nodes W_2 and W_4, causing a disruption of the contacts in W5-M1, W5-M2, W5-P1, W1-M11, W1-M15, W1-P3, W1-M16, and W1-P2. We assume that the control parameters before the disruption are $g = 2$, $\mu = 1.5$, $\Gamma = diag(5, 5, 5)$, $B_{ik} = diag[-0.5, -0.5, -0.5]$, $t = 0.05$, and the corresponding parameters for the cost are $K_g = 0.15$, $K_\mu = 0.1$, $K_\Gamma = 0.1$, $K_{Bik,} = 1$, $times = T/t = 6$. The above initial values continue to be used. Then, we get $R(0.3) = 0.7075$, cost = 5.95, $R_c(0.3) = 0.1189$.

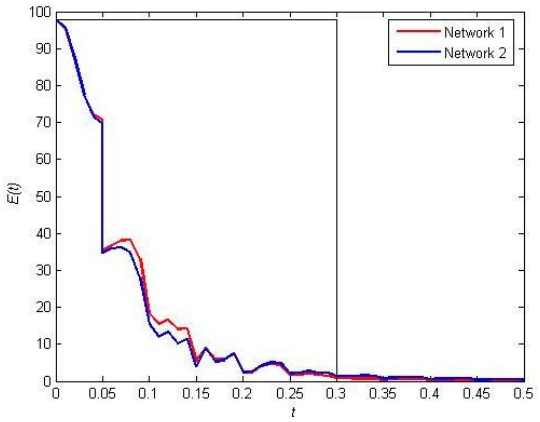

Figure 15. Comparison of the resilient recovery rate $R(t)$.

There are five kinds of recovery strategies (as shown in Section 4.2) to choose from. To further verify the method that helps to choose the resilient recovery strategy, the following two scenarios are designed.

Scenario 1: After the fire occurs, the emergency management ability, the strategy adjustment ability, the coupling node control ability, and the incentive mechanism of each enterprise remain unchanged. That is to say, the cost parameters of each strategy are not changed. We adopt the five strategies for the experiment. With different strategies, $\Delta g = 1$, $\Delta\mu = 1$, $\Delta\Gamma = 1$, $\Delta B_{ik,} = 0.1$. As shown in Table 5, the recovery rate, the cost, and the control efficiency are calculated.

Table 5. Scenario 1.

Scenario 1	Strategy	Strategy Parameter	Cost Parameter	Cost	$R(0.3)$	$R_C(0.3)$
Strategy 1	Emergency management	Δg = 1	Kg = 0.15	C = C0 + Kg*Δg = 6.10	0.7509	0.1231
Strategy 2	Strategy adjustment	Δμ = 1	Kμ = 0.1	C = C0 + Kμ*Δμ = 6.05	0.7091	0.1172
Strategy 3	Coupled node control	ΔΓ = 1	KΓ = 0.1	C = C0 = +KΓ*ΔΓ = 6.05	0.7075	0.1169
Strategy 4	Incentive mechanism	ΔBik, = 0.1	KBik, = 1	C = C0 = +KBik, *ΔBik, *T/t = 6.95	0.7264	0.1045
Strategy 5	Reconstruction	ΔRC = W1-P3	KRC = 1	C = C0 + KRC *ΔRC = 6.95	0.7086	0.1018
		ΔRC = W1-P2	KRC = 1	C = C0 + KRC *ΔRC = 6.95	0.7080	0.1017

In scenario 1, the control efficiency of emergency management measures is the highest. In strategy 5, recovering the backbone link W_1-P_3 has higher control efficiency than recovering the redundant link W_1-P_2, although the recovery cost is the same.

Scenario 2: After the fire, the cost parameters of the incentive system are reduced rather than increased when employees voluntarily work overtime to restore enterprise operations. The emergency management capability, strategy adjustment capability, and coupling node control capability of each enterprise remain unchanged. That is to say, the corresponding cost parameters of each strategy stay constant. As shown in Table 6, the control efficiency of the incentive mechanism is the highest in scenario 2.

Table 6. Scenario 2.

	Strategy	Strategy Parameter	Cost Parameter	Cost	$R(0.3)$	$R_C(0.3)$
Strategy 4	Incentive mechanism	$\Delta B_{ik,}$ = 0.1	$K_{Bik,}$ = 0.5	$C = C_0 = +K_{Bik,} *\Delta B_{ik,} *T/t$ = 3.95	0.7264	0.1839

From the above discussion, it can be seen that the proposed method can help supply chain managers to select the appropriate control strategies.

6. Conclusions

In the face of disruption, the question of how to obtain better control over resilient recovery of the supply network is an important problem. Using outer synchronization, efficient control and measurement for resilient recovery has been proposed. The conclusions are as follows:

(1) A dynamic SN model is established. The effective range of the resilient recovery method is given in Theorem 1.
(2) The measurement with memory for resilient recovery is proposed by the synchronization error. This method takes into account both time and speed.
(3) A greedy algorithm is designed to identify the backbone of the SN for the resilient recovery accordingly. It is very important to control the network backbone for resilient recovery.
(4) Certain common control strategies correspond to the parameters in our model, such as the incentive mechanism corresponding to the intensity of impulsive control, and the strategy adjustment corresponding to the capability of parameter identification.

In this paper, the control and measurement for resilient recovery consider the effectiveness and the control cost, helping to make better decisions. This method can be applied to other networks, such as communication networks and infrastructure networks. Meanwhile, there are still some limitations in this study. The relationship with the network backbone should be further studied. Follow-up studies are needed to address these problems.

Author Contributions: Conceptualization, L.G. and R.X.; methodology, R.X.; software, L.G.; validation, L.G. and R.X.; formal analysis, L.G.; investigation, L.G.; resources, L.G.; data curation, L.G.; writing—original draft preparation, L.G.; writing—review and editing, L.G.; visualization, L.G.; supervision, R.X.; project administration, R.X.; funding acquisition, L.G. All authors have read and agreed to the published version of the manuscript.

Funding: This research was funded by the Hubei Ministry of Education Humanities Social Sciences Fund (No. 18Y063) and the National Natural Science Foundation of China (No. 51875220). The APC was funded by Hubei Ministry of Education Humanities Social Sciences Fund (No. 18Y063).

Conflicts of Interest: The authors declare no conflict of interest.

References

1. Subulan, K.; Baykasoğlu, A.; Özsoydan, F.B.; Taşan, A.S.; Selim, H. A case-oriented approach to a lead/acid battery closed-loop supply chain network design under risk and uncertainty. *J. Manuf. Syst.* **2015**, *37*, 340–361. [CrossRef]
2. Genc, E.; Duffie, N.; Reinhart, G. Event-based supply chain early warning system for an adaptive production control. *Procedia CIRP* **2014**, *19*, 39–44. [CrossRef]
3. Jüttner, U.; Peck, H.; Christopher, M. Supply chain risk management: Outlining an agenda for future research. *Int. J. Logist.* **2003**, *6*, 197–210. [CrossRef]
4. Hosseini, S.; Al Khaled, A.; Sarder, M.D. A general framework for assessing system resilience using Bayesian networks: A case study of sulfuric acid manufacturer. *J. Manuf. Syst.* **2016**, *41*, 211–227. [CrossRef]
5. Fiksel, J.; Polyviou, M.; Croxton, K.L.; Pettit, T.J. From risk to resilience: Learning to deal with disruption. *MIT Sloan Manag. Rev.* **2015**, *56*, 79–86.
6. Fang, Y.P.; Pedroni, N.; Zio, E. Resilience-based component importance measures for critical infrastructure network systems. *IEEE Trans. Rel.* **2016**, *65*, 502–512. [CrossRef]
7. Rice, J.B.; Caniato, F. Building a secure and resilient supply network. *Supply Chain Manag. Rev.* **2003**, *7*, 22–30.
8. Hosseini, S.; Barker, K.; Ramirez-Marquez, J.E. A Review of Definitions and Measures of System Resilience. *Reliab. Eng. Syst. Saf.* **2015**, *145*, 47–61. [CrossRef]
9. Vugrin, E.D.; Camphouse, R.C. Infrastructure resilience assessment through control design. *Int. J. Crit. Infrastruct.* **2011**, *7*, 243–260. [CrossRef]
10. Liu, Y.; Slotine, J.; Barabási, A. Controllability of complex networks. *Nature* **2011**, *473*, 167–173. [CrossRef]
11. Zhou, L.; Wang, C.; He, H.; Lin, Y. Time-controllable combinatorial inner synchronization and outer synchronization of anti-star networks and its application in secure communication. *Commun. Nonlinear Sci.* **2015**, *22*, 623–640. [CrossRef]

12. Hohenstein, N.O.; Feisel, E.; Hartmann, E.; Giunipero, L. Research on the phenomenon of supply chain resilience: A systematic review and paths for further investigation. *Int. J. Phys. Distrib. Logist. Manag.* **2015**, *45*, 90–117. [CrossRef]
13. Barker, K.; Ramirez-Marquez, J.E.; Rocco, C.M. Resilience-based network component importance measures. *Reliab. Eng. Syst. Saf.* **2013**, *117*, 89–97. [CrossRef]
14. Fawcett, S.E.; Waller, M.A. Making sense out of chaos: Why theory is relevant to supply chain research. *J. Bus. Logist.* **2011**, *32*, 1–5. [CrossRef]
15. Fallah, H.; Eskandari, H.; Pishvaee, M.S. Competitive closed-loop supply chain network design under uncertainty. *J. Manuf. Syst.* **2015**, *37*, 649–661. [CrossRef]
16. Diabat, A.; Dehghani, E.; Jabbarzadeh, A. Incorporating location and inventory decisions into a supply chain design problem with uncertain demands and lead times. *J. Manuf. Syst.* **2017**, *43*, 139–149. [CrossRef]
17. Ponta, L.; Silvano, C. Traders' networks of interactions and structural properties of financial markets: An agent-based approach. *Complexity* **2018**, *2018*, 1–9. [CrossRef]
18. Hearnshaw, E.J.S.; Mark, M.J.W. A complex network approach to supply chain network theory. *Int. J. Oper. Prod. Manag.* **2013**, *33*, 442–469. [CrossRef]
19. Tang, H.; Chen, L.; Lu, J.A.; Chi, K.T. Adaptive synchronization between two complex networks with nonidentical topological structures. *Phys. A* **2008**, *387*, 5623–5630. [CrossRef]
20. Wu, X.; Zheng, W.X.; Zhou, J. Generalized outer synchronization between complex dynamical networks. *Chaos* **2009**, *19*, 013109. [CrossRef]
21. Lü, L.; Liu, S.; Li, G.; Zhao, G.; Gu, J.; Tian, J.; Wang, Z. Determination of configuration matrix element and outer synchronization among networks with different topologies. *Phys. A* **2016**, *461*, 833–839. [CrossRef]
22. Zhang, Q.; Luo, J.; Wan, L. Parameter identification and synchronization of uncertain general complex networks via adaptive-impulsive control. *Nonlinear Dyn.* **2014**, *71*, 353–359. [CrossRef]
23. Li, C.; Lü, L.; Sun, Y.; Wang, Y.; Wang, W.; Sun, A. Parameter identification and synchronization for uncertain network group with different structures. *Phys. A* **2016**, *457*, 624–631. [CrossRef]
24. Li, H.L.; Jiang, Y.L.; Wang, Z.; Zhang, L.; Teng, Z. Parameter identification and adaptive–impulsive synchronization of uncertain complex networks with nonidentical topological structures. *Optik* **2015**, *126*, 5771–5776. [CrossRef]
25. Wu, Z.; Fu, X. Outer synchronization between drive-response networks with nonidentical nodes and unknown parameters. *Nonlinear Dyn.* **2012**, *69*, 685–692. [CrossRef]
26. Ma, X.H.; Wang, J.A. Pinning outer synchronization between two delayed complex networks with nonlinear coupling via adaptive periodically intermittent control. *Neurocomputing* **2016**, *199*, 197–203. [CrossRef]
27. Liang, S.; Wu, R.; Chen, L. Adaptive pinning synchronization in fractional-order uncertain complex dynamical networks with delay. *Phys. A* **2015**, *444*, 49–62. [CrossRef]
28. Sun, W.; Chen, Z.; Lü, J.; Chen, S. Outer synchronization of complex networks with delay via impulse. *Nonlinear Dyn.* **2012**, *69*, 1751–1764. [CrossRef]
29. Lü, L.; Li, C.; Chen, L.; Zhao, G. New technology of synchronization for the uncertain dynamical network with the switching topology. *Nonlinear Dyn.* **2016**, *86*, 655–666. [CrossRef]
30. Geng, L.; Xiao, R. Outer synchronization and parameter identification approach to the resilient recovery of supply network with uncertainty. *Phys. A* **2017**, *482*, 407–421. [CrossRef]
31. Anne, K.R.; Chedjou, J.C.; Kyamakya, K. Bifurcation analysis and synchronisation issues in a three-echelon supply chain. *Int. J. Logist.* **2009**, *12*, 347–362. [CrossRef]
32. Göksu, A.; Kocamaz, U.E.; Uyarog˘lu, Y. Synchronization and control of chaos in supply chain management. *Comput. Ind. Eng.* **2015**, *86*, 107–115. [CrossRef]
33. Kocamaz, U.E.; Tas¸kın, H.; Uyarog˘lu, Y.; Göksu, A. Control and synchronization of chaotic supply chains using intelligent approaches. *Comput. Ind. Eng.* **2016**, *102*, 476–487. [CrossRef]
34. Lei, Z.; Li, Y.; Xu, Y. Chaos synchronization of bullwhip effect in a supply chain. In Proceedings of the 13th International Conference on Management Science and Engineering, Lille, France, 5–7 October 2006; pp. 557–560.
35. Ivanov, D.; Sokolov, B. Control and system-theoretic identification of the supply chain dynamics domain for planning, analysis, and adaptation of performance under uncertainty. *Eur. J. Oper. Res.* **2013**, *224*, 313–323. [CrossRef]

36. Zhang, J.; Wu, Z.; Hong, L.; Xu, X. Connectivity recovery of multi-agent systems based on connecting neighbor set. *Phys. A* **2011**, *390*, 4596–4601. [CrossRef]
37. Zhang, J.; Xu, X.; Hong, L.; Yan, Y. Consensus recovery of multi-agent systems subjected to failures. *Int. J. Control* **2012**, *85*, 280–286. [CrossRef]
38. Wang, G.; Cao, J.; Lu, J. Outer synchronization between two nonidentical networks with circumstance noise. *Phys. A* **2010**, *389*, 1480–1488. [CrossRef]
39. Tukamuhabwa, B.R.; Stevenson, M.; Busby, J.; Zorzini, M. Supply chain resilience: Definition, review and theoretical foundations for further study. *Int. J. Prod. Res.* **2015**, *53*, 5592–5623. [CrossRef]
40. Cimellaro, G.P.; Reinhorn, A.M.; Bruneau, M. Framework for analytical quantification of disaster resilience. *Eng. Struct.* **2010**, *32*, 3639–3649. [CrossRef]
41. Baroud, H.; Barker, K.; Ramirez-Marquez, J.E. Importance measures for inland waterway network resilience. *Transport. Res. E Logist.* **2014**, *62*, 55–67. [CrossRef]
42. Wei, X.; Chen, S.; Lu, J.A.; Ning, D. Reconstruction of complex networks with delays and noise perturbation based on generalized outer synchronization. *Phys. A* **2016**, *49*, 225101. [CrossRef]
43. Zhang, C.J.; Zeng, A. Network skeleton for synchronization: Identifying redundant connections. *Phys. A* **2014**, *402*, 180–185. [CrossRef]
44. Spiegler, V.L.M.; Naim, M.M.; Wikner, J. A control engineering approach to the assessment of supply chain resilience. *Int. J. Prod. Res.* **2012**, *50*, 6162–6187. [CrossRef]
45. Cardoso, S.R.; Barbosa-Póvoa, A.P.; Relvas, S.; Novais, A.Q. Resilience metrics in the assessment of complex supply-chains performance operating under demand uncertainty. *Omega Int. J. Manag.* **2015**, *56*, 53–73. [CrossRef]